arXiv:1110.3690v2 [nucl-ex] 31 Mar 2012

Search for double β decay processes in ^{106}Cd with the help of $^{106}CdWO_4$ crystal scintillator

P. Belli[a], R. Bernabei[a,b,1], R.S. Boiko[c], V.B. Brudanin[d], F. Cappella[e,f], V. Caracciolo[g,h], R. Cerulli[g], D.M. Chernyak[c], F.A. Danevich[c], S. d'Angelo[a,b], E.N. Galashov[i], A. Incicchitti[e,f], V.V. Kobychev[c], M. Laubenstein[g], V.M. Mokina[c], D.V. Poda[g,c], R.B. Podviyanuk[c], O.G. Polischuk[c], V.N. Shlegel[i], Yu.G. Stenin[i,2], J. Suhonen[j], V.I. Tretyak[c], Ya.V. Vasiliev[i]

[a] *INFN, Sezione di Roma "Tor Vergata", I-00133 Rome, Italy*
[b] *Dipartimento di Fisica, Università di Roma "Tor Vergata", I-00133 Rome, Italy*
[c] *Institute for Nuclear Research, MSP 03680 Kyiv, Ukraine*
[d] *Joint Institute for Nuclear Research, 141980 Dubna, Russia*
[e] *INFN, Sezione di Roma "La Sapienza", I-00185 Rome, Italy*
[f] *Dipartimento di Fisica, Università di Roma "La Sapienza", I-00185 Rome, Italy*
[g] *INFN, Laboratori Nazionali del Gran Sasso, I-67100 Assergi (AQ), Italy*
[h] *Dipartimento di Fisica, Università dell'Aquila, I-67100 L'Aquila, Italy*
[i] *Nikolaev Institute of Inorganic Chemistry, 630090 Novosibirsk, Russia*
[j] *Department of Physics, University of Jyväskylä, P.O. Box 35 (YFL), FI-40014 Finland*

Abstract

A search for the double β processes in ^{106}Cd was carried out at the Gran Sasso National Laboratories of the INFN (Italy) with the help of a $^{106}CdWO_4$ crystal scintillator (215 g) enriched in ^{106}Cd up to 66%. After 6590 h of data taking, new improved half-life limits on the double beta decay processes in ^{106}Cd were established at the level of $10^{19} - 10^{21}$ yr; in particular, $T_{1/2}^{2\nu\varepsilon\beta^+} \geq 2.1 \times 10^{20}$ yr, $T_{1/2}^{2\nu2\beta^+} \geq 4.3 \times 10^{20}$ yr, and $T_{1/2}^{0\nu2\varepsilon} \geq 1.0 \times 10^{21}$ yr. The resonant neutrinoless double electron captures to the 2718 keV, 2741 keV and 2748 keV excited states of ^{106}Pd are restricted to $T_{1/2}^{0\nu2K} \geq 4.3 \times 10^{20}$ yr, $T_{1/2}^{0\nu KL_1} \geq 9.5 \times 10^{20}$ yr and $T_{1/2}^{0\nu KL_3} \geq 4.3 \times 10^{20}$ yr, respectively (all limits at 90% C.L.). A possible resonant enhancement of the $0\nu2\varepsilon$ processes is estimated in the framework of the QRPA approach. The radioactive contamination of the $^{106}CdWO_4$ crystal scintillator is reported.

PACS: 29.40.Mc, 23.40.-s

Keywords: Double beta decay, ^{106}Cd, $CdWO_4$ crystal scintillator, Low counting experiment

[1] Corresponding author. *E-mail address:* rita.bernabei@roma2.infn.it (R. Bernabei).
[2] Deceased

1 INTRODUCTION

The neutrinoless double beta decay ($0\nu2\beta$) is a powerful tool to investigate the properties of the neutrino and of the weak interactions. The study of this nuclear decay, forbidden in the framework of the Standard Model, can allow us to determine an absolute scale of the neutrino mass and its hierarchy, to establish the nature of the neutrino (Majorana or Dirac particle), and to check the lepton number conservation, the possible contribution of right-handed admixture to the weak interaction, and the existence of Nambu-Goldstone bosons (majorons) [1].

Experimental efforts over the last seventy years have concentrated mainly on the decay modes with emission of two electrons. Allowed in the Standard Model, the two neutrino (2ν) $2\beta^-$ decay mode was observed in ten isotopes with half-lives in the range of $10^{18} - 10^{24}$ yr. For the $0\nu2\beta^-$ decay mode half-life limits at the level of $10^{23} - 10^{25}$ yr were set for several nuclei (see reviews [2, 3] and original studies [4, 5, 6, 7, 8, 9]), while positive evidence for ^{76}Ge has been published in [10] and new experiments are in progress to further investigate this latter isotope as well.

The results of the searches for the capture of two electrons from atomic shells (2ε), electron capture with positron emission ($\varepsilon\beta^+$), and emission of two positrons ($2\beta^+$) are at the level of $10^{16} - 10^{21}$ yr (see review [2] and original works [11, 12, 13, 14, 15, 16, 17, 18, 19, 20, 21, 22, 23, 24, 25, 26, 27]); although allowed, the two neutrino mode of these processes has not yet been detected[3]. High sensitivity experiments to search for neutrinoless 2ε and $\varepsilon\beta^+$ decays are also important because they could clarify a contribution of right-handed admixtures in weak interactions [31].

The isotope ^{106}Cd (the decay scheme is presented in Fig. 1) is among the most widely studied $2\beta^+$ nuclides thanks to the large energy release ($Q_{2\beta} = 2775.39(10)$ keV [32]) and to the comparatively high natural abundance ($1.25 \pm 0.06\%$ [33]). It should be stressed that ^{106}Cd is a rather promising isotope also according to the theoretical predictions [31, 34, 35, 36, 37, 38]. In particular, the calculated half-lives for the two neutrino mode of the 2ε and $\varepsilon\beta^+$ processes are at the level of $T_{1/2} \sim 10^{20} - 10^{22}$ yr [35, 39, 40, 41, 42], reachable with the present low counting technique.

Furthermore, in the case of the 0ν capture of two electrons from the K shell (or L and K shells), the energy releases of 2727 keV ($2K$ capture), 2747 keV (KL_1) and 2748 keV (KL_3) are close to the energies of a few excited levels of ^{106}Pd (with $E_{exc} = 2718$ keV, 2741 keV and 2748 keV). Such a coincidence could give a resonant enhancement of the $0\nu2\varepsilon$ capture [43, 44, 45, 46, 47, 48].

Therefore, it is not surprising that the study of ^{106}Cd has a rather long history. The half-life limits at the level of 10^{15} yr could be extracted from the old (1952) underground measurements of a Cd sample with photographic emulsions [49], while a search for positrons emitted in $2\beta^+$ decay was performed in 1955 with a Wilson cloud chamber in a magnetic field and with 30 g of cadmium foil; this gave a limit of 10^{16} yr [50]. Measurements of a 153 g Cd sample during 72 h with two NaI(Tl) scintillators working in coincidence have been carried out in [51]; the half-life limits at the level of $\sim 10^{17}$ yr were determined for $2\beta^+$, $\varepsilon\beta^+$ and 2ε processes.

The subsequent studies can be divided into two groups: experiments using samples of cadmium with external detectors for the detection of the emitted particles (with enriched

[3] An indication for $2\beta^+$ decay processes in ^{130}Ba was obtained by the geochemical method [28, 29]; however, this result has to be confirmed in a direct counting experiment. It is worth mentioning the work [30] where BaF_2 crystal scintillators were used to search for double β processes in ^{130}Ba.

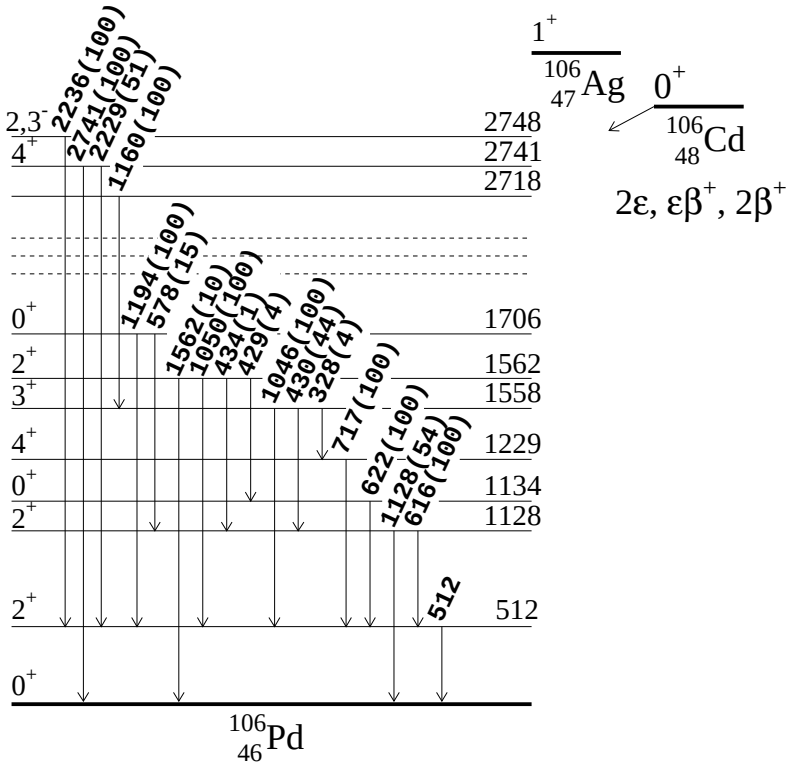

Figure 1: Simplified decay scheme of ^{106}Cd [52] (levels at $1904 - 2714$ keV are omitted). The energies of the excited levels and of the emitted γ quanta are in keV (relative intensities of γ quanta are given in parentheses).

^{106}Cd [22, 53] and natural cadmium [39]), and experiments with detectors containing cadmium, namely semiconductor CdTe and CdZnTe detectors [54, 55] and $CdWO_4$ crystal scintillators [7, 56, 57]. Previous experiments on the searches for the 2β processes in ^{106}Cd are summarized in Table 1.

Data from the experiment, performed in the Solotvina Underground Laboratory (1000 m w.e.), with a 15 cm^3 $^{116}CdWO_4$ crystal scintillator (enriched in ^{116}Cd to 83%, with 0.16% of ^{106}Cd), were used to set the limits on the 2β decay of ^{106}Cd at the level of $10^{17} - 10^{19}$ yr [56]. In experiment [39], 331 g of Cd foil were measured at the Frejus Underground Laboratory (4800 m w.e.) with a 120 cm^3 HPGe detector during 1137 h; γ quanta from the annihilations of the positrons and from the de-excitation of the daughter ^{106}Pd nucleus were searched for, giving rise to half-life limits at the level of $10^{18} - 10^{19}$ yr. In [57], a large (1.046 kg) $CdWO_4$ scintillator was measured at the Gran Sasso National Laboratories (3600 m w.e.) over 6701 h. The determined limits on the half-life for the $2\beta^+$ and $\varepsilon\beta^+$ decays were at the level of $\sim 10^{19}$ yr for 0ν, and $\sim 10^{17}$ yr for 2ν processes. A small (0.5 g) CdTe crystal was tested as a cryogenic bolometer in 1997 [54]; the achieved sensitivity was $\sim 10^{16}$ yr for $0\nu 2\beta^+$ decay. An experiment [53] was performed in 1999 at the Gran Sasso National Laboratories using an enriched ^{106}Cd (to 68%) cadmium sample (154 g) and two low background NaI(Tl) scintillators installed in the low background DAMA/R&D set-up during 4321 h; these measurements reached a sensitivity level of more than 10^{20} yr for $2\beta^+$, $\varepsilon\beta^+$ and 2ε processes. A long-term (14183 h) experiment in the Solotvina Underground Laboratory with enriched $^{116}CdWO_4$ scintillators (total mass of 330

g) was completed in 2003 [7]; in addition, results of dedicated measurements during 433 h with a 454 g not-enriched $CdWO_4$ crystal were also considered [58]. In general, the experimental sensitivity was improved by approximately one order of magnitude in comparison with the older measurements [56].

There are two running experiments to search for 2β decay of ^{106}Cd: COBRA and TGV-II. The $T_{1/2}$ limits in the range of $10^{17} - 10^{18}$ yr were set in the COBRA experiment [55] using CdTe and CdZnTe crystals. In the TGV-II experiment [22, 23], 32 planar HPGe detectors are used. Cadmium foils enriched in ^{106}Cd to 75% are inserted between neighbouring detectors. The main goal of the TGV experiment is the search for the two neutrino double electron capture in ^{106}Cd. After 8687 h plus 12900 h (in two phases of the experiment) of data taking, the limits on double β decay of ^{106}Cd to the ground state and to the excited levels of ^{106}Pd are around 10^{20} yr.

Table 1: Experiments on the searches for the 2β decay of ^{106}Cd. The range of the $T_{1/2}$ limits corresponds to values given for the transitions to the ground state or to the excited levels of ^{106}Pd. More detailed information can be found in the original papers (see also [2]). COBRA and TGV experiments are still running.

Description	$T_{1/2}$ **limit, yr**	**Year [Ref.]**
Cd samples between photographic emulsions[a]	$\sim 10^{15}$ ($0\nu2\beta^+$, $0\nu\varepsilon\beta^+$)	1952 [49]
Cd foil in a Wilson cloud chamber	6×10^{16} ($0\nu2\beta^+$)	1955 [50]
Cd sample between two NaI(Tl) scintillators in coincidence	$(2.2 - 2.6) \times 10^{17}$ ($2\beta^+$) $(4.9 - 5.7) \times 10^{17}$ ($\varepsilon\beta^+$) 1.5×10^{17} ($2\nu2\varepsilon$)	1984 [51]
$^{116}CdWO_4$ crystal scintillator	$(0.5 - 1.4) \times 10^{18}$ ($0\nu2\beta^+$) $(0.3 - 1.1) \times 10^{19}$ ($0\nu\varepsilon\beta^+$) $5.8{\times}10^{17}$ ($2\nu2\varepsilon$)	1995 [56]
$CdWO_4$ crystal scintillator	2.2×10^{19} ($0\nu2\beta^+$) 9.2×10^{17} ($2\nu2\beta^+$) 5.5×10^{19} ($0\nu\varepsilon\beta^+$) 2.6×10^{17} ($2\nu\varepsilon\beta^+$)	1996 [57]
Cd sample measured by HPGe detector	1.0×10^{19} ($2\beta^+$) $(6.6 - 8.1) \times 10^{18}$ ($\varepsilon\beta^+$) $(3.5 - 6.2) \times 10^{18}$ (2ε)	1996 [39]
CdTe cryogenic bolometer	1.4×10^{16} ($0\nu\varepsilon\beta^+$)	1997 [54]
^{106}Cd sample between two NaI(Tl) scintillators in coincidence	$(1.6{-}2.4){\times}10^{20}$ ($2\beta^+$) $(1.1 - 4.1) \times 10^{20}$ ($\varepsilon\beta^+$) $(3.0 - 7.3) \times 10^{19}$ (2ε)	1999 [53]
$^{116}CdWO_4$ crystal scintillators	$(0.5 - 1.4) \times 10^{19}$ ($2\beta^+$) $(0.1 - 7.0) \times 10^{19}$ ($\varepsilon\beta^+$) $(0.6 - 8.0) \times 10^{18}$ (2ε)	2003 [7]
CdZnTe semiconductor detectors (COBRA)	$(0.9 - 2.7) \times 10^{18}$ ($2\beta^+$) $(4.6 - 4.7) \times 10^{18}$ ($\varepsilon\beta^+$) 1.6×10^{17} (2ε)	2009 [55]
^{106}Cd samples between planar HPGe detectors (TGV)	3.6×10^{20} ($2\nu2\varepsilon$) 1.1×10^{20} ($0\nu2\varepsilon$, 2741 keV)	2011 [22]
	$(1.4 - 1.7) \times 10^{20}$ ($2\beta^+$) $(1.1 - 1.6) \times 10^{20}$ ($\varepsilon\beta^+$) 1.6×10^{20} ($0\nu2\varepsilon$, 2718 keV)	2011 [23]

[a] To our knowledge, this was the first underground experiment in history of investigations of 2β decay.

We would like to mention two important advantages of the experiments using detectors containing cadmium: a higher detection efficiency for the different channels of the ^{106}Cd double β decay, and a possibility to resolve the two neutrino and the neutrinoless modes of the decay.

Thanks to their good scintillation characteristics, their low level of intrinsic radioactivity, and their pulse-shape discrimination ability (which allows an effective reduction of the background), cadmium tungstate crystal scintillators were successfully applied to low background experiments in order to search for the double β decay of the cadmium and tungsten isotopes [7, 16, 57], and in order to investigate rare α [59] and β [58, 60] decays.

The aim of the present work was the search for the 2β processes in ^{106}Cd with the help of a low background cadmium tungstate crystal scintillator enriched in ^{106}Cd ($^{106}CdWO_4$).

2 EXPERIMENT

The cadmium tungstate crystal (27 mm in diameter by 50 mm in length; mass 215 g), used in the experiment, was developed [61] from deeply purified cadmium [62] enriched in ^{106}Cd to 66%. The scintillator was fixed inside a cavity ($\oslash 47 \times 59$ mm) in the central part of a polystyrene light-guide, 66 mm in diameter by 312 mm in length. The cavity was filled with high purity silicon oil. Two high purity quartz light-guides, 66 mm in diameter by 100 mm in length, were optically connected to the opposite sides of the polystyrene light-guide. To collect the scintillation light the assembly was viewed by two low radioactive EMI9265–B53/FL, 3" diameter photomultiplier tubes (PMT). The detector was installed deep underground in the low background DAMA/R&D set-up at the Gran Sasso National Laboratories of the INFN (Italy). It was surrounded by copper bricks and sealed in a low radioactive, air-tight copper box continuously flushed with high purity nitrogen gas to avoid the presence of residual environmental radon. The copper box was surrounded by a passive shield made of high purity copper, 10 cm of thickness, 15 cm of low radioactive lead, 1.5 mm of cadmium and 4 to 10 cm of polyethylene/paraffin to reduce the external background. The shield was contained inside a Plexiglas box, also continuously flushed with high purity nitrogen gas.

An event-by-event data acquisition system recorded the amplitude, the arrival time, and the pulse shape of the events by means of a 1 GS/s 8 bit DC270 Transient Digitizer by Acqiris (adjusted to a sampling frequency of 20 MS/s) over a time window of 100 μs.

The energy resolution of the detector was measured with ^{22}Na, ^{60}Co, ^{133}Ba, ^{137}Cs, ^{228}Th, and ^{241}Am γ sources in the beginning of the experiment. For instance, the energy resolution (full width at half maximum, FWHM) of the $^{106}CdWO_4$ detector for the γ quanta of ^{137}Cs (662 keV) and of ^{228}Th (2615 keV) was 14.2(3)% and 8.4(2)%, respectively. Two additional calibration measurements were performed: one approximately in the middle, and the second one at the end of the experiment with the help of ^{22}Na, ^{60}Co, ^{137}Cs, and ^{228}Th γ sources to test the detector stability. In addition, the energy scale of the detector was checked by using the peaks due to ^{207}Bi contamination of the $^{106}CdWO_4$ crystal scintillator (see Section 3.4). The energy scale during the experiment was reasonably stable with a deviation in the range of $(1-2)$%. The data of the calibration measurements were used to estimate the dependence of the energy resolution on the energy. Below 500 keV the energy resolution of the detector to γ quanta with energy E_γ can be described by the function: $\mathrm{FWHM}_\gamma = \sqrt{11.2 \times E_\gamma}$, while above 500 keV the data are fitted by $\mathrm{FWHM}_\gamma = \sqrt{-4900 + 21 \times E_\gamma}$, where FWHM_γ and E_γ are given in keV.

The low background measurements were carried out in three runs listed in Table 2. The energy interval of the data taking was chosen as $0.05 - 4$ MeV in Run 1 to investigate the background of the detector at low energy. Taking into account the rather high activity of β active $^{113}Cd^m$ (see the next Section), the data acquisition was slightly modified in order to avoid the recording of the pulse shapes of all events with an energy lower than 0.4 MeV (Run 2); the upper energy threshold was ≈ 1.8 MeV. In a third run, after some improvement in the data acquisition system, the energy threshold was increased to ≈ 0.57 MeV and the upper energy threshold was set to 4 MeV (Run 3). The data accumulated in Run 2 were used to estimate the activity of ^{228}Th in the $^{106}CdWO_4$ crystal by a time-amplitude analysis (see Section 3.1). The first 1320 h of data taking (Run 1 + part of Run 3) were already analyzed and presented in [63].

Table 2: The low background measurements with the $^{106}CdWO_4$ crystal scintillator. Times of measurements (t), energy intervals of data taking (ΔE), and background counting rates (BG) in different energy intervals are specified.

Run	t (h)	ΔE (MeV)	BG (counts/(yr×keV×kg)) in energy interval (MeV)		
			$0.8 - 1.0$	$2.0 - 2.9$	$3.0 - 4.0$
1	283	$0.05 - 4.0$	474(18)	2.6(6)	0.4(3)
2	2864	$0.40 - 1.8$	453(11)	–	–
3	6307	$0.57 - 4.0$	412(4)	2.3(1)	0.33(4)

3 DATA ANALYSIS

The energy spectrum accumulated with the $^{106}CdWO_4$ detector in Runs 1 and 3 over 6590 h is presented in Fig. 2. The counting rate ≈ 24 counts/s below the energy ≈ 0.65 MeV is mainly due to the β decay of $^{113}Cd^m$ with activity 116(4) Bq/kg. Contamination of the enriched ^{106}Cd by the β active $^{113}Cd^m$ has been found in the low background TGV experiment [64], where β particles and X rays from thin foils of the enriched ^{106}Cd were measured by planar Ge detectors; part of this material was used to produce the $^{106}CdWO_4$ crystal.

Contributions to the background above the energy ≈ 0.6 MeV were analyzed by means of the time-amplitude and of the pulse-shape discrimination techniques, as well as by the fit of the data with Monte Carlo simulated models of the background.

3.1 Time-amplitude analysis of ^{228}Th activity

The arrival time and the energy of each event were used to select the events of the fast decay chain in the ^{232}Th family[4]: ^{224}Ra ($Q_\alpha = 5.79$ MeV, $T_{1/2} = 3.66$ d) $\rightarrow$ ^{220}Rn ($Q_\alpha = 6.41$ MeV, $T_{1/2} = 55.6$ s) $\rightarrow$ ^{216}Po ($Q_\alpha = 6.91$ MeV, $T_{1/2} = 0.145$ s) $\rightarrow$ ^{212}Pb. To select α events from the decays of ^{224}Ra, ^{220}Rn, and ^{216}Po, one should take into account the quenching of the scintillation output in the $CdWO_4$ crystal scintillator, the so called α/β ratio, defined as the

[4]The technique of the time-amplitude analysis is described in detail e.g. in [65, 66].

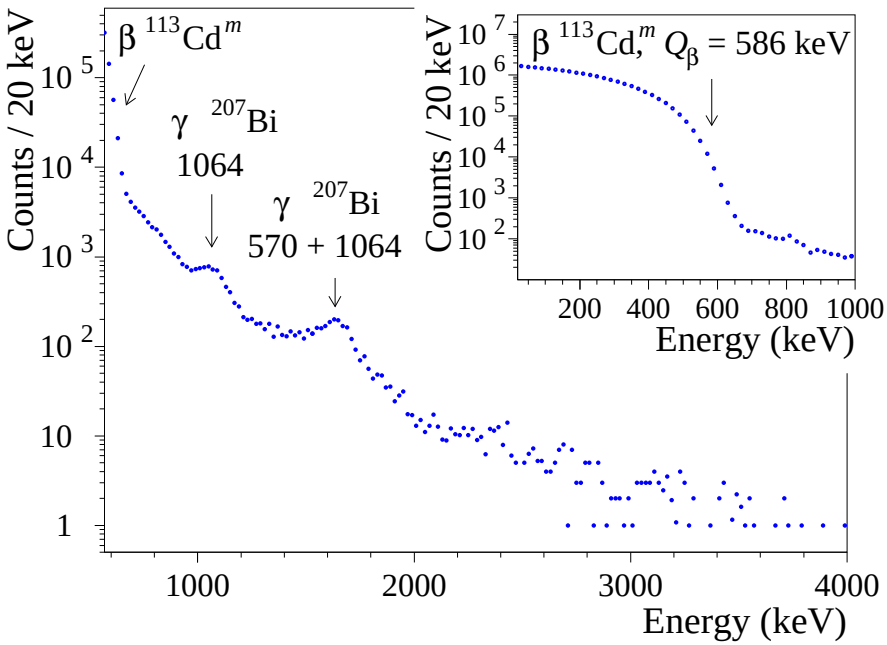

Figure 2: (Color online) The energy spectrum measured with the $^{106}CdWO_4$ scintillator over 6590 h in the low background set-up. (Inset) The decay of the β active $^{113}Cd^m$ dominates at the energy < 0.65 MeV (the data over 283 h).

ratio of an α peak position in the γ scale of a detector to the energy of the alpha particles. The dependence of the α/β ratio on the energy of the α particles measured for $^{116}CdWO_4$ scintillator [59]: $\alpha/\beta = 0.083(9) + 0.0168(13) \times E_\alpha$ (where E_α is in MeV), was used to estimate the positions of ^{224}Ra, ^{220}Rn, and ^{216}Po α peaks in the data accumulated with the $^{106}CdWO_4$ detector. As a first step, all the events within an energy interval $0.6 - 1.8$ MeV were used as triggers, while for the second events a time interval $0.026 - 1.45$ s and the same energy window were required. Taking into account the efficiency of the events selection in this time interval (88.2% of ^{216}Po decays), the activity of ^{228}Th in the $^{106}CdWO_4$ crystal was calculated to be 0.042(4) mBq/kg. As a next step, all the selected pairs (^{220}Rn – ^{216}Po) were used as triggers in order to find the events of the decay of the mother α active ^{224}Ra. A $1.45 - 111$ s time interval (73.2% of ^{220}Rn decays) was chosen to select events in the energy interval $0.6 - 1.75$ MeV. The obtained α peaks from the ^{224}Ra$\rightarrow^{220}$Rn$\rightarrow^{216}$Po$\rightarrow^{212}$Pb chain and the time distributions for the ^{220}Rn$\rightarrow^{216}$Po and ^{216}Po$\rightarrow^{212}$Pb decays are shown in Fig. 3.

The positions of the three α peaks, selected by the time-amplitude analysis in the γ scale of the detector, were used to obtain the following dependence of the α/β ratio on the energy of the α particles, E_α, in the range $5.8 - 6.9$ MeV: $\alpha/\beta = 0.11(2) + 0.011(3) \times E_\alpha$ (where E_α is in MeV). The dependence is in agreement with the data obtained for the $^{116}CdWO_4$ scintillation detector in [59].

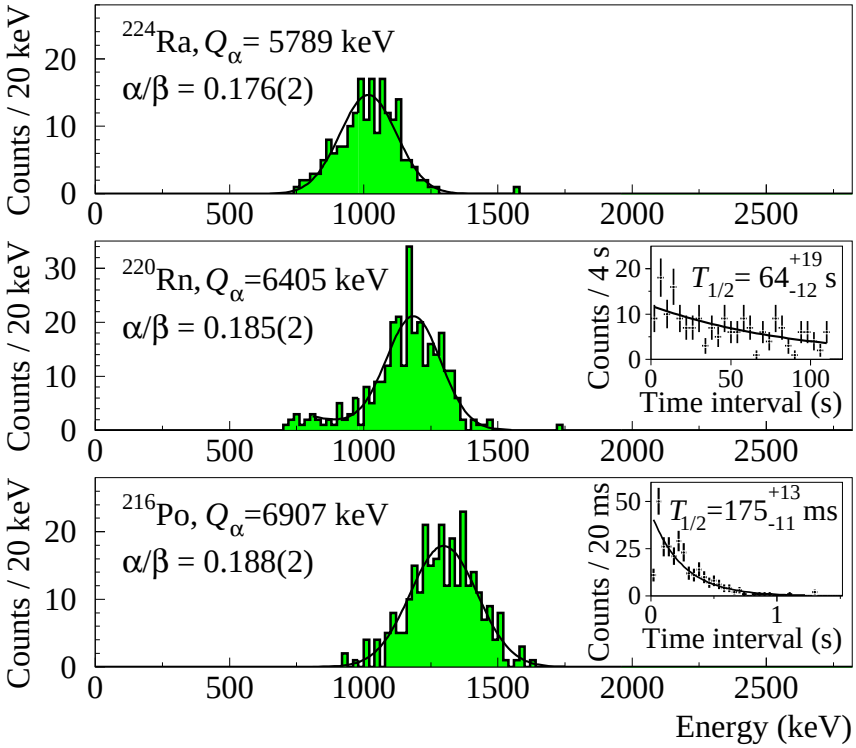

Figure 3: (Color online) Alpha peaks of ^{224}Ra, ^{220}Rn and ^{216}Po selected by the time-amplitude analysis from the data accumulated over 9454 h with the $^{106}CdWO_4$ detector. The obtained half-lives of ^{220}Rn (64^{+19}_{-12} s) and ^{216}Po (175^{+13}_{-11} ms) are in agreement with the table values (55.6 s and 145 ms, respectively [67]).

3.2 Pulse-shape discrimination

As demonstrated in [68], the difference in pulse shapes in the $CdWO_4$ scintillator can be used to discriminate $\gamma(\beta)$ events from those induced by α particles. The optimal filter method proposed by E. Gatti and F. De Martini in 1962 [69] was applied for this purpose. For each signal $f(t)$, the numerical characteristic of its shape (shape indicator, SI) was defined as: $SI = \sum f(t_k) \times P(t_k) / \sum f(t_k)$. There the sum is over the time channels k, starting from the origin of signal and averaging up to 50 μs, and $f(t_k)$ is the digitized amplitude (at the time t_k) of a given signal. The weight function $P(t)$ was defined as: $P(t) = \{f_\alpha(t) - f_\gamma(t)\}/\{f_\alpha(t) + f_\gamma(t)\}$, where $f_\alpha(t)$ and $f_\gamma(t)$ are the reference pulse shapes for α particles and γ quanta measured in [70]. By using this approach, α events were clearly separated from $\gamma(\beta)$ events as shown in Fig. 4 where the scatter plot of the shape indicator versus energy is depicted for the data of the low background measurements with the $^{106}CdWO_4$ detector. The distribution of the shape indicators for events with energies in the range $0.7-1.4$ MeV (shown in Inset of Fig. 4) justifies reasonable pulse-shape discrimination between α particles and γ quanta (β particles), as well as a possibility to reject randomly overlapped pulses (mainly caused by the β decay of $^{113}Cd^m$).

The energy spectrum of the α events selected with the help of the pulse-shape discrimination is shown in Fig. 5. As demonstrated in [59], the energy resolution for the α particles is worse than that for the γ quanta due to the dependence of the α/β ratio on the direction of the

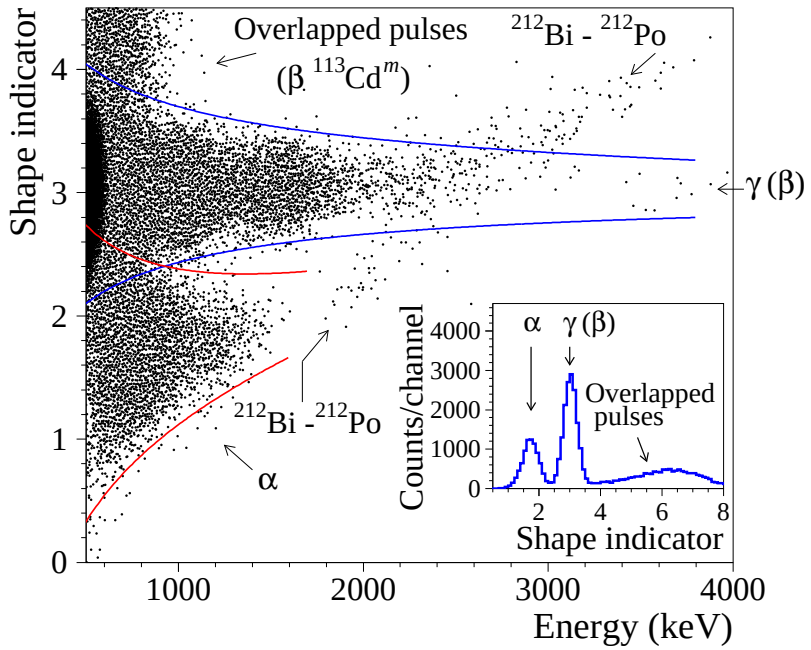

Figure 4: (Color online) The shape indicators (see text) versus the energy accumulated over 6590 h with the $^{106}CdWO_4$ crystal scintillator in the low background set-up. Three sigma intervals for shape indicator values corresponding to γ quanta (β particles) and α particles are depicted. Events with shape indicator values greater than ≈ 3.8 can be explained by the overlap of events (mainly of β decays of $^{113}Cd^m$ in the crystal), while the population of the events in the energy interval $\approx 1.8 - 3.8$ MeV with shape indicators outside of the $\gamma(\beta)$ region are due to the decays of the fast ^{212}Bi – ^{212}Po sub-chain of ^{228}Th. (Inset) The distribution of the shape indicators demonstrates the efficiency of the pulse-shape discrimination between $\gamma(\beta)$, α and overlapped pulses.

α particles relative to the $CdWO_4$ crystal axes[5]. As a result we cannot definitively identify single U/Th α active daughters in the spectrum. Therefore, we set only limits on α activities of U/Th daughters in the $^{106}CdWO_4$ crystal scintillator. For this purpose, the spectrum was fitted in the energy interval $550 - 1500$ keV by a simple model, built of Gaussian functions (to describe the α peaks of U/Th daughters) plus an exponential function to describe the background. The activities of ^{228}Th and ^{226}Ra were restricted taking into account the results of the time-amplitude and of the double pulse (see Section 3.3) analyses. The fit and its components are shown in Fig. 5. The limits on the activity of the U/Th daughters (supposing a broken equilibrium in the chains) are presented in Table 3. The total α activity of U/Th in the $^{106}CdWO_4$ crystal is 2.1(2) mBq/kg.

The pulse-shape analysis also allows us to distinguish the main part of the ^{212}Bi$\rightarrow^{212}$Po$\rightarrow^{208}$Pb events from the trace contamination of the crystal by ^{228}Th (see Fig. 4).

[5]One could compare the energy resolutions of the α peaks presented in Fig. 3 with the expected resolution for γ quanta (see Section 2).

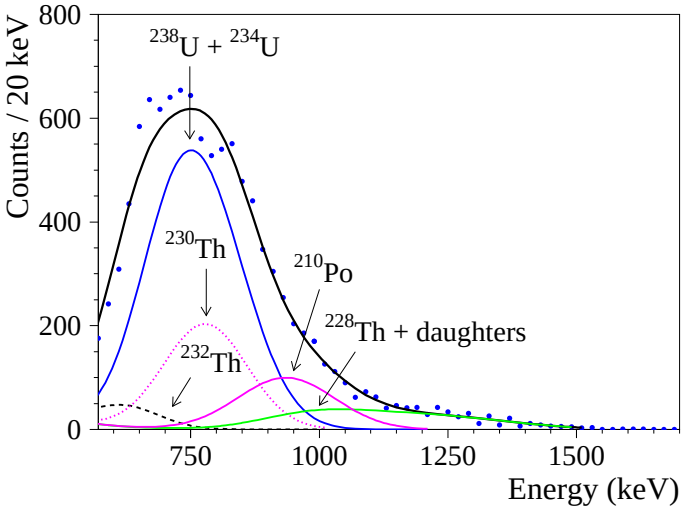

Figure 5: (Color online) The energy distribution of the α events (points) selected by the pulse-shape analysis from the data accumulated over 6590 h with the $^{106}CdWO_4$ detector together with the fit (solid line) by a model, which includes the α decays from ^{232}Th and ^{238}U families.

3.3 Identification of Bi-Po events

The search for the fast decays ^{214}Bi ($Q_\beta = 3.27$ MeV, $T_{1/2} = 19.9$ m) $\rightarrow$ ^{214}Po ($Q_\alpha = 7.83$ MeV, $T_{1/2} = 164$ μs) $\rightarrow$ ^{210}Pb (in equilibrium with ^{226}Ra from the ^{238}U chain) was performed with the help of the pulse-shape analysis of the double pulses[6]. Only eleven ^{214}Bi – ^{214}Po events were found in the data over 6590 h. Taking into account the detection efficiency in the time window of $1 - 50$ μs (it contains 18.6% of the ^{214}Po decays), one can estimate the activity of ^{226}Ra in the $^{106}CdWO_4$ crystal as 0.012(3) mBq/kg.

To select double pulses produced by the fast chain of the decays ^{212}Bi ($Q_\beta = 2.25$ MeV, $T_{1/2} = 60.55$ m) $\rightarrow$ ^{212}Po ($Q_\alpha = 8.95$ MeV, $T_{1/2} = 0.299$ μs) $\rightarrow$ ^{208}Pb (in equilibrium with ^{228}Th from the ^{232}Th family), a front edge analysis was developed (see also [59]). The energy spectrum of the selected ^{212}Bi – ^{212}Po events and the time distribution of ^{212}Po decay are presented in Fig. 6. The approach gives the activity of ^{228}Th as 0.051(4) mBq/kg, in a reasonable agreement with the result of the time-amplitude analysis.

All the selected Bi-Po events were removed from the $\gamma(\beta)$ spectrum of the $^{106}CdWO_4$ detector.

3.4 Simulation of the $\gamma(\beta)$ background, radioactive contamination of $^{106}CdWO_4$ scintillator

To reproduce the background of the $^{106}CdWO_4$ detector, we consider the contribution of the primordial radioactive isotopes ^{40}K and ^{238}U/^{232}Th with their daughters, anthropogenic radionuclides ^{90}Sr-^{90}Y and ^{137}Cs, and cosmogenic ^{106}Ru and ^{110m}Ag. Anthropogenic ^{90}Sr and ^{137}Cs are the most widespread radionuclides, in particular after the Chernobyl accident. Contamination of cadmium tungstate by ^{106}Ru and ^{110m}Ag was estimated in [72], while presence of

[6]The technique of the analysis is described e.g. in [59, 71].

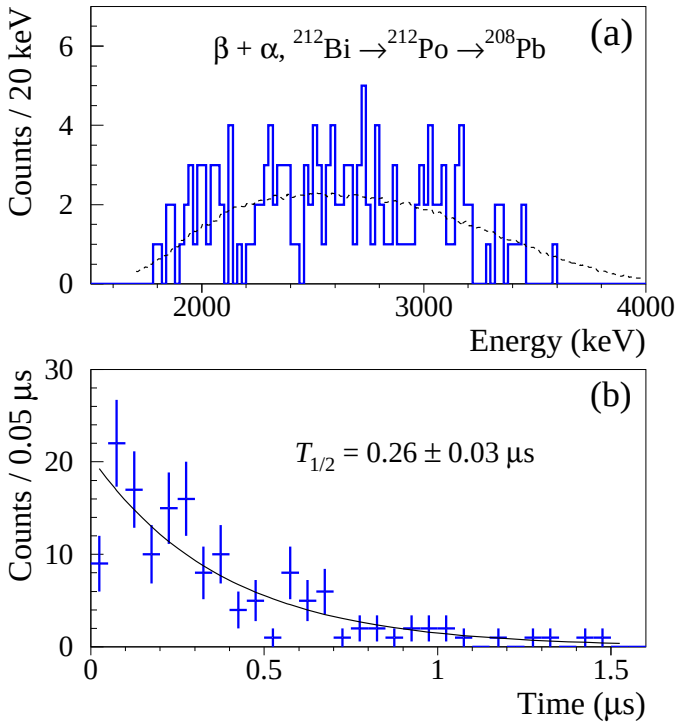

Figure 6: (Color online) (a) The energy spectrum of ^{212}Bi→^{212}Po→^{208}Pb events in the ^{106}CdWO$_4$ scintillator selected by means of the pulse-shape and of the front edge analyses (see text) from the data accumulated over 6590 h together with the fit (dashed line) of the simulated distribution. (b) The time distribution of the ^{212}Po α decay selected by the front edge analysis. The fit of the time distribution gives a half-life: $T_{1/2} = (0.26 \pm 0.03)$ μs, in agreement with the table value for ^{212}Po (0.299 μs [67]).

^{110m}Ag in ^{116}CdWO$_4$ crystal scintillators was observed in [73]. The radioactive contamination of the set-up (in particular the PMTs and the copper box) can contribute to the background, too. The energy distributions of the possible background components were simulated with the help of the EGS4 [74] and GEANT4 [75] codes. The initial kinematics of the particles emitted in the nuclear decays was given by the event generator DECAY0 [76].

The background energy spectrum of the γ and β events, selected by means of the pulse-shape, of the front edge and of the double pulse analyses, was fitted by a model built from the simulated distributions. The activities of the U/Th daughters were bounded taking into account the results of the time-amplitude and of the pulse-shape analyses. The activities of the ^{40}K, ^{232}Th and ^{238}U in the PMTs were taken from [77]. The radioactive contaminations of the copper box have been assumed to be equal to those reported in [78]. In addition, we have added a model of the overlapped ^{113}Cd^m β decays, which contribute to the background in the energy region up to ≈ 1 MeV.

Two clear peculiarities in the spectrum of the CdWO$_4$ detector at (1064 ± 3) keV and at (1631 ± 5) keV cannot be explained by the contribution from the external γ quanta. Indeed, no similar peaks were observed in the low background measurements with radiopure ZnWO$_4$ crystal scintillators [79] performed before the present experiment in the same experimental conditions.

To explain the peculiarities, we suppose a pollution of the crystal by ^{207}Bi ($T_{1/2}$ = 31.55 yr, Q_{EC} = 2398 keV [67]). The presence of ^{207}Bi could be caused by the contamination of the facilities at the Nikolaev Institute of Inorganic Chemistry (Novosibirsk, Russia) where the $^{106}CdWO_4$ crystal was grown. A large amount of BGO crystal scintillators is in production in that laboratory. BGO crystal scintillators are typically contaminated by ^{207}Bi at the level of 0.01 – 10 Bq/kg [80, 81, 82, 83]. Moreover, we cannot also exclude the possibility of a $^{106}CdWO_4$ crystal surface contamination in the laboratory of the Institute for Nuclear Research (Kyiv, Ukraine) where the scintillator was diffused and preliminary tested [61] with several gamma sources, including an open ^{207}Bi source. Therefore, two distributions of ^{207}Bi (uniformly distributed in the crystal volume and deposited on its surface) were also simulated and added to the background model.

A fit of the spectrum of $\gamma(\beta)$ events in the energy region 0.66 – 4.0 MeV by the model described above, and by the main components of the background are shown in Fig. 7. The fit (χ^2/n.d.f. = 111/108 = 1.03, where n.d.f. is number of degrees of freedom) confirmed more likely a surface contamination of the crystal scintillator by ^{207}Bi at level of 3 mBq (0.06 mBq/cm^2). We cannot distinguish the part of the activity due to bulk contamination and we give only a limit on the internal contamination of the crystal by ^{207}Bi as $\leq$ 0.7 mBq/kg.

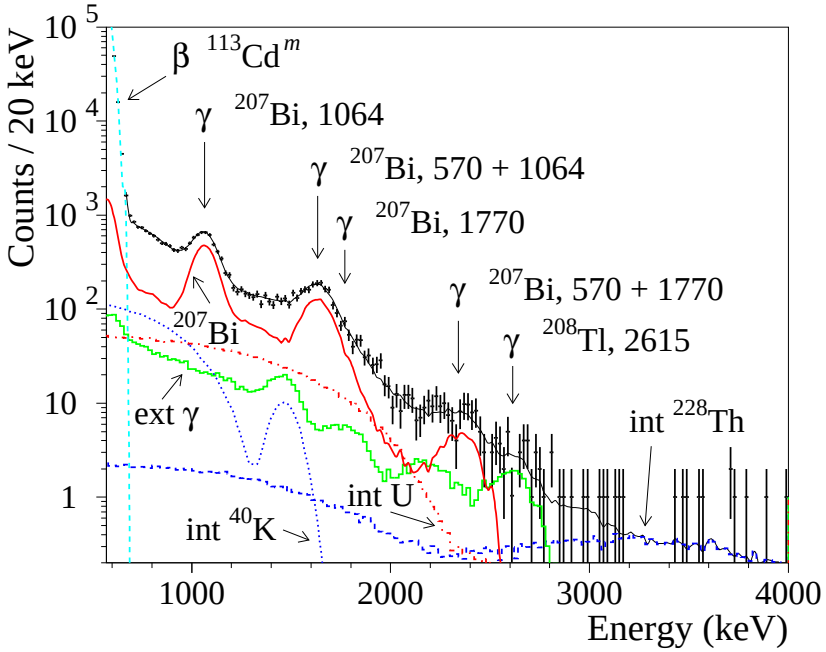

Figure 7: (Color online) The energy spectrum of the $\beta(\gamma)$ events accumulated over 6590 h in the low background set-up with the $^{106}CdWO_4$ crystal scintillator (points) together with the background model (black continuous superimposed line). The main components of the background are shown: the β spectrum of the internal $^{113}Cd^m$, the distributions of ^{40}K, ^{228}Th, ^{238}U, ^{207}Bi (deposited on the crystal surface), and the contribution from the external γ quanta from PMTs and copper box ("ext γ") in these experimental conditions.

There are no other clear peculiarities in the spectrum which could be ascribed to the internal trace radioactive contamination. Therefore, we just set limits on the activities of ^{40}K, ^{90}Sr-^{90}Y,

cosmogenic ^{106}Ru and ^{110m}Ag. A summary of radioactive contamination of the $^{106}CdWO_4$ crystal scintillator is given in Table 3. We hope to clarify further the radioactive contamination of the scintillator at a next stage of the experiment by running the $^{106}CdWO_4$ crystal scintillator in coincidence/anti-coincidence with an ultra-low background HPGe γ detector.

Table 3: Radioactive contamination of the $^{106}CdWO_4$ scintillator determined by different methods (activities are presented in mBq/kg, while the surface contamination by ^{207}Bi is given in mBq/cm^2). Data for $^{116}CdWO_4$ and $CdWO_4$ crystal scintillators are presented for comparison.

Chain	Nuclide	Activity		
		$^{106}CdWO_4$	$^{116}CdWO_4$ [59, 7, 73]	$CdWO_4$ [57, 60]
^{232}Th	^{232}Th	≤ 0.07 [a]	$\leq 0.08 - 0.053(9)$	≤ 0.026
	^{228}Th	0.042(4) [b]	$0.039(2) - 0.062(6)$	$\leq (0.003 - 0.014)$
^{238}U	^{238}U	≤ 0.6 [a]	$\leq (0.4 - 0.6)$	≤ 1.3
	^{230}Th	≤ 0.4 [a]	$\leq (0.05 - 0.5)$	
	^{226}Ra	0.012(3) [c]	≤ 0.005	$\leq (0.007 - 0.018)$
	^{210}Po	≤ 0.2 [a]	$\leq (0.063 - 0.6)$	≤ 0.063
Total α activity		2.1(2) [a]	$1.4(1) - 2.7(3)$	0.26(4)
	^{40}K	≤ 1.4 [d]	≤ 0.4	$\leq (1.7 - 5)$
	^{90}Sr-^{90}Y	≤ 0.3 [d]	≤ 0.2	≤ 1
	^{106}Ru	≤ 0.02 [d]	–	–
	^{110m}Ag	≤ 0.06 [d]	0.06(4)	–
	^{113}Cd	182 [e]	91(5)	$558(4) - 580(20)$
	^{113}Cd^m	116000(4000) [d]	0.43(6)	$\leq 3.4 - 150(10)$
	^{137}Cs	–	2.1(5)	≤ 0.3
	^{207}Bi internal	≤ 0.7 [d]	0.6(2)	–
	^{207}Bi surface	0.06 [d]	–	–

[a] Pulse-shape discrimination (Section 3.2)
[b] Time-amplitude analysis (Section 3.1)
[c] Analysis of double pulses (Section 3.3)
[d] Fit of the background spectrum (Section 3.4)
[e] Calculated taking into account the isotopic abundance of ^{113}Cd in $^{106}CdWO_4$ [61] and the half-life of ^{113}Cd [60].

4 RESULTS AND DISCUSSION

There are no peculiarities in the data accumulated with the $^{106}CdWO_4$ detector which could be ascribed to the double β decay of ^{106}Cd. Therefore only lower half-life limits can be set by using the formula:

$$\lim T_{1/2} = N \times \eta \times t \times \ln 2 / \lim S,$$

where N is the number of ^{106}Cd nuclei in the $^{106}CdWO_4$ crystal (2.42×10^{23}), η is the detection efficiency, t is the time of measurements, and $\lim S$ is the number of events of the effect searched for, which can be excluded at a given confidence level (C.L.; all the limits on the double beta processes in ^{106}Cd are given at 90% C.L. in the present study).

The response functions of the $^{106}CdWO_4$ detector to the 2β processes in ^{106}Cd were simulated with the help of the EGS4 [74] and the DECAY0 [76] packages (some examples of the simulated spectra are presented in Fig. 8).

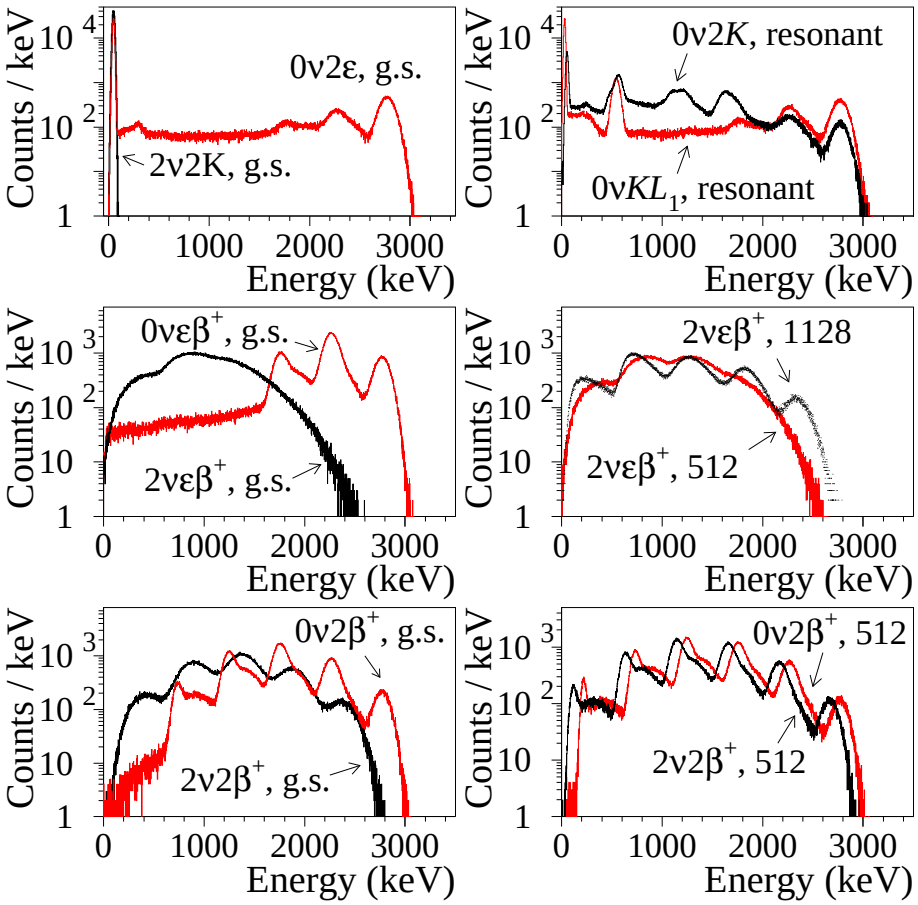

Figure 8: (Color online) Simulated response functions of the $^{106}CdWO_4$ detector to 2ε, $\varepsilon\beta^+$ and $2\beta^+$ processes in ^{106}Cd.

4.1 Double beta processes in ^{106}Cd with positron(s) emission

To estimate the value of $\lim S$ for the $2\nu\varepsilon\beta^+$ decay of ^{106}Cd to the ground state of ^{106}Pd, the energy spectrum of the γ and β events accumulated over 6590 h with the $^{106}CdWO_4$ detector was fitted by the model built from the components of the background (see Section 3.4) and the effect searched for. The activities of U/Th daughters in the crystals were constrained in the fit taking into account the results of the time-amplitude and pulse-shape analyses. The initial values of the ^{40}K, ^{232}Th and ^{238}U activities inside the PMTs were taken from [77], where the radioactive contaminations of PMTs of the same model were measured. The radioactive

contaminations of the copper were constrained taking into account the data of the measurements [84] where copper of a similar quality was used. The best fit (achieved in the energy interval $780 - 2800$ keV with $\chi^2/\text{n.d.f.} = 93/81 = 1.15$) gives an area of the $2\nu\varepsilon\beta^+$ distribution in the interval of the fit: (26 ± 230) counts, thus with no evidence for the effect. In accordance with the Feldman-Cousins procedure [85], this corresponds to $\lim S = 403$ counts at 90% C.L. Taking into account the detection efficiency within the fit window given by the Monte Carlo simulation ($\eta = 0.700$) and the 98% efficiency of the pulse-shape discrimination to select $\gamma(\beta)$ events, we get the following limit on the decay:

$$T_{1/2}^{2\nu\varepsilon\beta^+}(\text{g.s.} \to \text{g.s.}) \geq 2.1 \times 10^{20} \text{ yr} \qquad \text{at 90\% C.L.}$$

The excluded energy distribution expected for the two neutrino $\varepsilon\beta^+$ decay of ^{106}Cd is shown in Fig. 9.

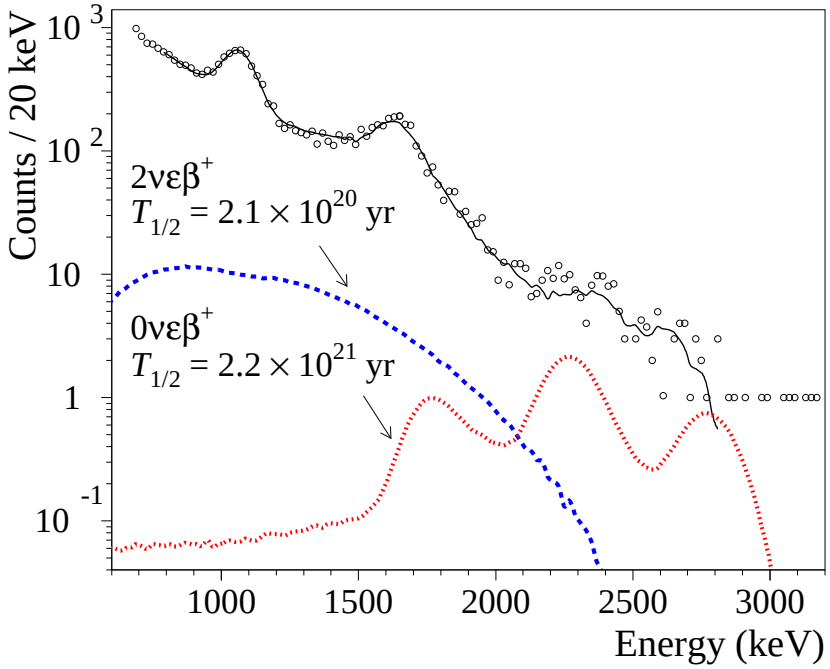

Figure 9: (Color online) Part of the energy spectrum of γ and β events accumulated with the $^{106}CdWO_4$ detector over 6590 h (circles) and its fit in the energy interval $780 - 2800$ keV (solid line) together with the excluded distributions of $2\nu\varepsilon\beta^+$ and $0\nu\varepsilon\beta^+$ decay of ^{106}Cd.

One can prove this result by using the so called "one sigma" approach when a value of $\lim S$ can be estimated as the square root of the counts in the energy interval of interest. There are 5462 events in the energy interval $1140 - 2220$ keV where the detection efficiency for the $2\nu\varepsilon\beta^+$ decay is 36%. The method gives a limit $T_{1/2}^{2\nu\varepsilon\beta^+} \geq 6.0 \times 10^{20}$ yr at 68% C.L., similar to the result acquired by fitting the experimental data with the help of the Monte Carlo simulated models.

The sensitivity to the neutrinoless channel of the $\varepsilon\beta^+$ decay is better thanks to the shift of the energy distribution to higher energies. Moreover, there are clear peaks in the spectrum of the $0\nu\varepsilon\beta^+$ process in the energy region $1.6 - 2.9$ MeV, which make the effect much more

distinguishable (see Fig. 9). A fit of the data in the energy interval 2000−3000 keV (χ^2/n.d.f. = 23/25 = 0.92) gives an area of the effect (17 ± 13) events ($\lim S = 38$ events, $\eta = 0.675$), which corresponds to the following limit on the $0\nu\varepsilon\beta^+$ decay of ^{106}Cd to the ground state of ^{106}Pd:

$$T_{1/2}^{0\nu\varepsilon\beta^+}(\text{g.s.} \to \text{g.s.}) \geq 2.2 \times 10^{21} \text{ yr} \qquad \text{at } 90\% \text{ C.L.}$$

The "one sigma" approach gives for this decay the limit (there are 187 events in the energy interval $2140 - 2960$ keV, where the detection efficiency for the $0\nu\varepsilon\beta^+$ decay is 62%): $T_{1/2}^{0\nu\varepsilon\beta^+} \geq 5.6 \times 10^{21}$ yr at 68% C.L., proving the result obtained by fitting the experimental data.

A fit of the data in the energy interval $1200 - 3000$ keV (χ^2/n.d.f. = 71/65 = 1.09) gives $S = (92 \pm 52)$ events ($\lim S = 177$ events, $\eta = 0.616$) of the $2\nu2\beta^+$ decay of ^{106}Cd to the ground level of ^{106}Pd. Therefore, we set the following limit:

$$T_{1/2}^{2\nu2\beta^+}(\text{g.s.} \to \text{g.s.}) \geq 4.3 \times 10^{20} \text{ yr} \qquad \text{at } 90\% \text{ C.L.}$$

The neutrinoless double positron decay was restricted by the fit in the energy interval $760 - 2800$ keV (χ^2/n.d.f. = 88/82 = 1.07, $S = -14 \pm 69$, $\lim S = 100$, $\eta = 0.956$):

$$T_{1/2}^{0\nu2\beta^+}(\text{g.s.} \to \text{g.s.}) \geq 1.2 \times 10^{21} \text{ yr} \qquad \text{at } 90\% \text{ C.L.}$$

It should be stressed that the mass difference between ^{106}Cd and ^{106}Pd atoms also allows transitions to the excited levels of ^{106}Pd. Thus, we have given limits on the $2\beta^+$ decay of ^{106}Cd to the first excited level of ^{106}Pd (2^+, 512 keV), and on the electron capture with positron emission to a few lowest excited levels of ^{106}Pd with the spin-parity 0^+ and 2^+. The results are presented in Table 4.

4.2 Double electron capture in ^{106}Cd

In the case of 2ν double electron capture in ^{106}Cd from the K or/and L shells the total energy release in the $^{106}CdWO_4$ detector is in the range from $2E_{L3} = 6.3$ keV to $2E_K = 48.8$ keV (where E_K and E_L are the binding energies of the electrons on the K and L shells of the palladium atom, respectively). Detection of such an energy deposit requires a low enough energy threshold and low background conditions. In our measurements the energy threshold for the acquisition was set too high (because of the background due to the β decay of $^{113}Cd^m$) to search for the two neutrino mode of double electron capture to the ground state and to the first excited level of ^{106}Pd.

However, we can analyze the existing data to search for the 2ν double electron capture to the higher excited levels of ^{106}Pd. For instance, by fitting the background spectrum in the energy interval $660 - 2780$ keV (χ^2/n.d.f. = 103/86 = 1.20, $S = -5 \pm 63$, $\lim S = 99$, $\eta = 0.328$) the following half-life limit on $2\nu2\varepsilon$ decay of ^{106}Cd to the 2_2^+ level (1128 keV) of ^{106}Pd was obtained:

$$T_{1/2}^{2\nu2\varepsilon}(\text{g.s.} \to 2_2^+) \geq 4.1 \times 10^{20} \text{ yr} \qquad \text{at } 90\% \text{ C.L.}$$

The following restriction was set on the $2\nu2\varepsilon$ decay of ^{106}Cd to the 0_1^+ 1134 keV level of ^{106}Pd by fitting the experimental spectrum in the energy interval 660–2800 (χ^2/n.d.f. = 105/87 = 1.21, $S = -5 \pm 163$, $\lim S = 263$, $\eta = 0.367$):

$$T_{1/2}^{2\nu 2\varepsilon}(g.s. \to 0_1^+) \geq 1.7 \times 10^{20} \text{ yr} \qquad \text{at } 90\% \text{ C.L.}$$

In the case of the neutrinoless double electron capture, different particles can be emitted: X rays and Auger electrons from de-excitations in atomic shells, γ quanta and/or conversion electrons from de-excitation of daughter nucleus. We suppose here that only one γ quantum is emitted in the nuclear de-excitation process. It should be stressed that the electron captures from different shells ($2K$, KL, $2L$ and other modes) cannot be energetically resolved by our detector. The fit of the measured spectrum in the energy interval $1800-3200$ keV (χ^2/n.d.f. $= 37/41 = 0.90$, $S = 7 \pm 10$, $\lim S = 23$, $\eta = 0.194$) gives the following limit on the $0\nu 2\varepsilon$ transition of ^{106}Cd to the ground state of ^{106}Pd:

$$T_{1/2}^{0\nu 2\varepsilon}(\text{g.s.} \to \text{g.s.}) \geq 1.0 \times 10^{21} \text{ yr} \qquad \text{at } 90\% \text{ C.L.}$$

The limits on the double electron capture in ^{106}Cd to the lowest excited levels of ^{106}Pd were obtained by a fit of the data in different energy intervals (see Table 4).

4.3 Resonant neutrinoless double electron capture in ^{106}Cd

A resonant neutrinoless double electron capture in ^{106}Cd is possible on three excited levels of ^{106}Pd with energies 2718 keV, 2741 keV and 2748 keV.

The half-life of the ^{106}Cd resonant 2ε process was estimated [86] by using the general formalism of [87] and by calculating the associated nuclear matrix element in a realistic single-particle space with a microscopic nucleon-nucleon interaction. We have used a higher-RPA (random-phase approximation) framework called the multiple-commutator model (MCM) [88, 89]. Using the UCOM short-range correlations [90], the half-life for the 0ν double electron capture in ^{106}Cd to the 2718 keV level of ^{106}Pd (assuming its spin-parity is 0^+) can be written as:

$$T_{1/2} = (3.0 - 8.1) \times 10^{22} \times \frac{x^2+26.2}{\langle m_\nu \rangle^2} \text{ yr} \qquad (1)$$

where $x = |Q_{2\beta} - E|$, and $\langle m_\nu \rangle$ (the effective Majorana neutrino mass) are in eV units. Here $Q_{2\beta}$ is the difference in atomic masses between ^{106}Cd and ^{106}Pd, and E contains the nuclear excitation energy and the hole energies in the atomic s orbitals. The dependence of the half-life on x is plotted in Fig. 10 for several values of $\langle m_\nu \rangle$. Use of the the recently remeasured (by the Penning-trap mass spectrometry [32]) value of $Q_{2\beta}$ leads to a value $x = 8390$ eV for the degeneracy parameter, and thus to the 2ε half-life estimate: $T_{1/2} = (2.1 - 5.7) \times 10^{30}$ yr for $\langle m_\nu \rangle = 1$ eV.

We have estimated limits on the resonant $0\nu 2K$ and $0\nu KL$ processes in ^{106}Cd by using the data from our experiment. For instance, the fit of the energy spectrum of the γ and β events measured by the $^{106}CdWO_4$ detector over 6590 h in the energy region $1280 - 3000$ keV ($\eta = 0.315$) gives 35 ± 34 events for the 0ν double electron captures from two K shells to the excited level at 2718 keV. We should take $\lim S = 91$ events, which leads to the following limit on the possible resonant process:

$$T_{1/2}^{0\nu 2K}(\text{g.s.} \to 2718 \text{ keV}) \geq 4.3 \times 10^{20} \text{ yr} \qquad \text{at } 90\% \text{ C.L.}$$

For the 0ν double electron capture of K and L_1 electrons to the level 2741 keV we have obtained a slightly stronger restriction ($S = 10 \pm 13$, $\lim S = 31$, $\eta = 0.238$):

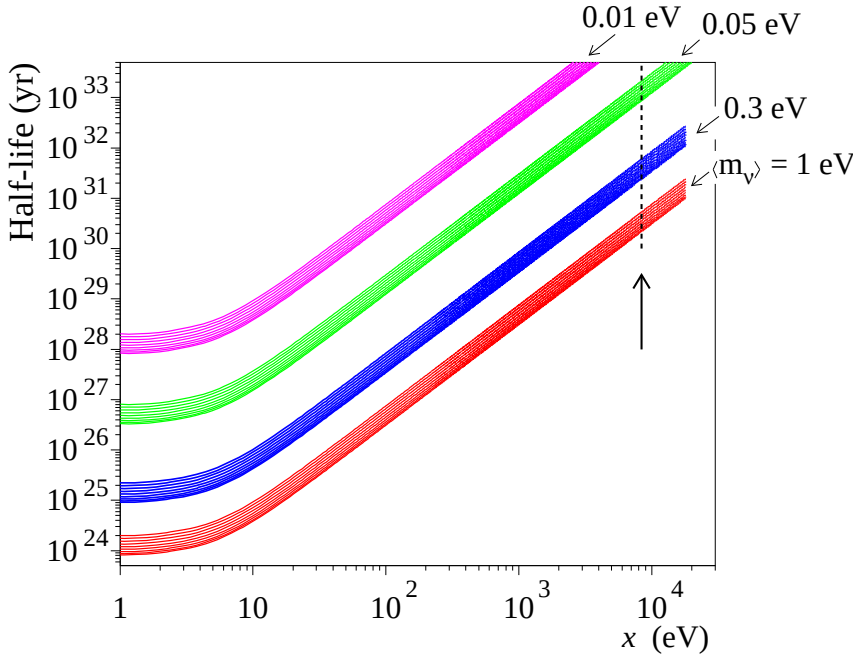

Figure 10: (Color online) Calculated half-life for the resonant $0\nu 2\varepsilon$ capture decay of ^{106}Cd to the excited level 2718 keV of ^{106}Pd as a function of parameter x (see text) for different values of the effective neutrino mass. Dashed line and arrow show the value of x derived from the recent measurements of the $Q_{2\beta}$ in ^{106}Cd [32].

$$T_{1/2}^{0\nu KL_1}(\text{g.s.} \to 2741 \text{ keV}) \geq 9.5 \times 10^{20} \text{ yr} \qquad \text{at } 90\% \text{ C.L.}$$

However, one can expect that the $0\nu KL$ process is strongly suppressed due to the large spin (4^+) of the level at 2741 keV.

Finally, for the 0ν double electron capture of K and L_3 electrons to the $2, 3^-$ level at 2748 keV we have obtained the following limit ($S = 35 \pm 21$, $\lim S = 69$, $\eta = 0.238$):

$$T_{1/2}^{0\nu KL_3}(\text{g.s.} \to 2748 \text{ keV}) \geq 4.3 \times 10^{20} \text{ yr} \qquad \text{at } 90\% \text{ C.L.}$$

Despite the fact that the limits are far away from the theoretical predictions, they are higher than the existing limits and are at the level of the best restrictions on resonant processes reported for different isotopes. The limit for the 0ν double electron capture to the level at 2748 keV is obtained for the first time.

All the half-life limits on 2β decay of ^{106}Cd obtained in the present work are summarized in Table 4 where results of the most sensitive previous studies are given for comparison.

Although the obtained bounds are well below the existing theoretical predictions [31, 34, 35, 36, 37, 38], most of the limits are about one order of magnitude higher than those previously established. Moreover, some channels of ^{106}Cd double β decay were investigated for the first time. It should be stressed that only two nuclides (^{78}Kr [21] and ^{130}Ba [28]) among six potentially $2\beta^+$ active isotopes [2] were investigated at a comparable level of sensitivity $T_{1/2} \sim 10^{21}$ yr.

Table 4: Half-life limits on 2β processes in ^{106}Cd. The detection efficiencies for the effect searched for (η) and the values of $\lim S$ within the energy intervals of fit (ΔE) are presented.

Decay channel	Decay mode	Level of ^{106}Pd (keV)	ΔE (keV)	η	$\lim S$	$T_{1/2}$ limit (yr) at 90% C.L.	
						Present work	Best previous limits
2ε	2ν	g.s.	–	–	–	–	$\geq 3.6 \times 10^{20}$ [22]
		2_1^+ 512	–	–	–	–	$\geq 1.2 \times 10^{20}$ [23]
		2_2^+ 1128	660 – 2780	0.328	99	$\geq 4.1 \times 10^{20}$	$\geq 5.1 \times 10^{18}$ [39]
		0_1^+ 1134	660 – 2800	0.367	263	$\geq 1.7 \times 10^{20}$	$\geq 1.0 \times 10^{20}$ [23]
		2_3^+ 1562	660 – 2800	0.342	830	$\geq 5.1 \times 10^{19}$	–
		0_2^+ 1706	760 – 2800	0.320	370	$\geq 1.1 \times 10^{20}$	–
		0_3^+ 2001	760 – 2780	0.484	208	$\geq 2.9 \times 10^{20}$	–
		0_4^+ 2278	660 – 3000	0.381	294	$\geq 1.6 \times 10^{20}$	–
	0ν	g.s.	1800 – 3200	0.194	23	$\geq 1.0 \times 10^{21}$	$\geq 8.0 \times 10^{18}$ [7]
		2_1^+ 512	2040 – 3200	0.150	36	$\geq 5.1 \times 10^{20}$	$\geq 3.5 \times 10^{18}$ [39]
		2_2^+ 1128	760 – 3000	0.465	187	$\geq 3.1 \times 10^{20}$	$\geq 4.9 \times 10^{19}$ [53]
		0_1^+ 1134	760 – 3000	0.474	169	$\geq 3.5 \times 10^{20}$	$\geq 7.3 \times 10^{19}$ [53]
		2_3^+ 1562	760 – 3000	0.520	186	$\geq 3.5 \times 10^{20}$	–
		0_2^+ 1706	760 – 3000	0.531	262	$\geq 2.5 \times 10^{20}$	–
		0_3^+ 2001	1300 – 3200	0.346	185	$\geq 2.3 \times 10^{20}$	–
		0_4^+ 2278	660 – 3200	0.564	335	$\geq 2.1 \times 10^{20}$	–
Res. $2K$	0ν	2718	1280 – 3000	0.315	91	$\geq 4.3 \times 10^{20}$	$\geq 1.6 \times 10^{20}$ [23]
Res. KL_1		4^+ 2741	1280 – 3000	0.238	31	$\geq 9.5 \times 10^{20}$	$\geq 1.1 \times 10^{20}$ [22]
Res. KL_3		$2, 3^-$ 2748	1300 – 3000	0.238	69	$\geq 4.3 \times 10^{20}$	–
$\varepsilon\beta^+$	2ν	g.s.	780 – 2800	0.700	403	$\geq 2.1 \times 10^{20}$	$\geq 4.1 \times 10^{20}$ [53]
		2_1^+ 512	660 – 3000	0.846	943	$\geq 1.1 \times 10^{20}$	$\geq 2.6 \times 10^{20}$ [53]
		2_2^+ 1128	1260 – 3000	0.414	167	$\geq 3.1 \times 10^{20}$	$\geq 1.4 \times 10^{20}$ [53]
		0_1^+ 1134	1200 – 3000	0.519	172	$\geq 3.7 \times 10^{20}$	$\geq 1.6 \times 10^{20}$ [23]
	0ν	g.s.	2000 – 3000	0.675	38	$\geq 2.2 \times 10^{21}$	$\geq 3.7 \times 10^{20}$ [53]
		2_1^+ 512	1200 – 3000	0.936	91	$\geq 1.3 \times 10^{21}$	$\geq 2.6 \times 10^{20}$ [53]
		2_2^+ 1128	1200 – 3000	0.678	148	$\geq 5.7 \times 10^{20}$	$\geq 1.4 \times 10^{20}$ [53]
		0_1^+ 1134	2000 – 3000	0.240	59	$\geq 5.0 \times 10^{20}$	$\geq 1.6 \times 10^{20}$ [23]
$2\beta^+$	2ν	g.s.	1200 – 3000	0.616	177	$\geq 4.3 \times 10^{20}$	$\geq 2.4 \times 10^{20}$ [53]
		2_1^+ 512	760 – 2800	0.831	203	$\geq 5.1 \times 10^{20}$	$\geq 1.7 \times 10^{20}$ [23]
	0ν	g.s.	760 – 2800	0.956	100	$\geq 1.2 \times 10^{21}$	$\geq 2.4 \times 10^{20}$ [53]
		2_1^+ 512	780 – 3000	0.870	92	$\geq 1.2 \times 10^{21}$	$\geq 1.7 \times 10^{20}$ [23]

A new phase of the experiment with the $^{106}CdWO_4$ scintillation detector placed in the ultra-low background GeMulti set-up (four HPGe detectors of 225 cm^3 volume each, located at the Gran Sasso National Laboratories) is in preparation. We are going to record pulse-profiles and arrival time of the events from the $^{106}CdWO_4$ scintillator both in coincidence and anti-coincidence modes. To suppress the background due to the radioactive contamination

of the PMT, the development of a lead tungstate ($PbWO_4$) active light-guide from ultra-pure archaeological lead [91, 62] has been completed. Our preliminary simulations show that such an experiment could investigate the 2ν mode of $\varepsilon\beta^+$ and of $2\beta^+$ decays, and also 2ε transitions of ^{106}Cd to the excited states of ^{106}Pd, at a level of sensitivity near to the theoretical predictions: $T_{1/2} \sim 10^{20} - 10^{22}$ yr [31, 34, 35, 36, 37, 38].

Moreover, the development of a $^{106}CdWO_4$ crystal scintillator depleted in the ^{113}Cd isotope by a factor $10^3 - 10^4$ (to reduce the background caused by β decay of $^{113}Cd^m$) is also possible [92]. Such a detector could be able to investigate two neutrino double electron capture, which is theoretically the most favorable process of 2β decay of ^{106}Cd.

5 CONCLUSIONS

A low background experiment using radiopure cadmium tungstate crystal scintillator (215 g) enriched in ^{106}Cd to 66% has been carried out at the underground Gran Sasso National Laboratories of the INFN. The background of the detector below 0.65 MeV is mainly due to the β active $^{113}Cd^m$ ($\approx$ 116 Bq/kg). We have found surface contamination of the crystal by ^{207}Bi at level of 3 mBq, which provides a considerable part of the background up to $\approx$ 2.5 MeV. The activities of U/Th in the scintillator are rather low: $\approx$ 0.04 mBq/kg of ^{228}Th and $\approx$ 0.01 mBq/kg of ^{226}Ra. The total α activity of U/Th is at level of $\approx$ 2 mBq/kg. A background counting rate of the detector in the vicinity of the ^{106}Cd double beta decay energy ($2.7 - 2.9$ MeV), after rejection of ^{212}Bi – ^{212}Po events, is 0.4 counts/(yr×keV×kg).

After 6590 h of data taking, new improved limits on 2β decay of ^{106}Cd were set at level of $10^{19} - 10^{21}$ yr, in particular: $T_{1/2}^{2\nu\varepsilon\beta^+} \geq 2.1 \times 10^{20}$ yr, $T_{1/2}^{2\nu 2\beta^+} \geq 4.3 \times 10^{20}$ yr, and $T_{1/2}^{0\nu 2\varepsilon} \geq 1.0 \times 10^{21}$ yr. Resonant $0\nu 2\varepsilon$ processes have been restricted to: $T_{1/2}^{0\nu 2K}$(g.s. $\rightarrow$ 2718 keV) $\geq 4.3 \times 10^{20}$ yr; $T_{1/2}^{0\nu KL_1}$(g.s. $\rightarrow$ 2741 keV) $\geq 9.5 \times 10^{20}$ yr and $T_{1/2}^{0\nu KL_3}$(g.s. $\rightarrow$ 2748 keV) $\geq 4.3 \times 10^{20}$ yr (all the limits at 90% C.L.). A possible resonant enhancement of $0\nu 2\varepsilon$ processes was estimated in the framework of the QRPA approach. The half-life of the resonant decay depends on the difference between the value of $Q_{2\beta}$ and of the energies of the appropriate excited levels of ^{106}Pd minus the binding energies of two electrons on shells of the daughter atom. The half-life decreases with the decrease of this difference.

A next stage of the experiment is in preparation. We are going to install a low background scintillation detector with the $^{106}CdWO_4$ crystal into the GeMulti ultra-low background set-up with four 225 cm^3 HPGe detectors at the Gran Sasso National Laboratories. The sensitivity of the experiment, in particular to the two neutrino $\varepsilon\beta^+$ decay of ^{106}Cd, is expected to be enhanced thanks to the high energy resolution of the GeMulti detector and to the improvement of the background conditions in coincidence mode. In addition, we hope to reduce the surface contamination of the scintillator with ^{207}Bi, observed in the present study, by cleaning (removing) the crystal surface. We estimate the sensitivity of the experiment, in particular to the $2\nu\varepsilon\beta^+$ decay of ^{106}Cd, to be at level of the theoretical predictions $T_{1/2} \sim 10^{20} - 10^{22}$ yr.

Moreover, a further improvement of sensitivity can be reached by increasing the enrichment factor of ^{106}Cd, and by developing $^{106}CdWO_4$ scintillators with lower level of radioactive contaminations, including depletion in ^{113}Cd. A $^{106}CdWO_4$ scintillation detector with an activity of $^{113}Cd^m$ reduced by a factor of $10^3 - 10^4$ could be able to detect two neutrino double electron capture in ^{106}Cd, which is theoretically the most probable process.

6 ACKNOWLEDGMENTS

The group from the Institute for Nuclear Research (Kyiv, Ukraine) was supported in part by the Project "Kosmomikrofizyka-2" (Astroparticle Physics) of the National Academy of Sciences of Ukraine. D.V. Poda and O.G. Polischuk were supported in part by the Project "Double beta decay and neutrino properties" for young scientists of the National Academy of Sciences of Ukraine (Reg. No. 0110U004150). Authors would like to express their gratitude to the Referee for the careful reading of the manuscript and for the valuable comments.

References

[1] F.T. Avignone III, S.R. Elliott, and J. Engel, Rev. Mod. Phys. **80**, 481 (2008);
H.V. Klapdor-Kleingrothaus, Int. J. Mod. Phys. E **17**, 505 (2008);
H. Ejiri, J. Phys. Soc. Japan **74**, 2101 (2005);
F.T. Avignone III, G.S. King, and Yu.G. Zdesenko, New J. Phys. **7**, 6 (2005);
S.R. Elliot and J. Engel, J. Phys. G **30**, R183 (2004);
J.D. Vergados, Phys. Rep. **361**, 1 (2002);
S.R. Elliot and P. Vogel, Ann. Rev. Nucl. Part. Sci. **52**, 115 (2002);
Yu.G. Zdesenko, Rev. Mod. Phys. **74**, 663 (2002).

[2] V.I. Tretyak and Yu.G. Zdesenko, At. Data Nucl. Data Tables **61**, 43 (1995);
V.I. Tretyak and Yu.G. Zdesenko, At. Data Nucl. Data Tables **80**, 83 (2002).

[3] A.S. Barabash, Phys. At. Nucl. **73**, 162 (2010).

[4] H.V. Klapdor-Kleingrothaus et al., Eur. Phys. J. A **12**, 147 (2001).

[5] C.E. Aalseth et al., Phys. Rev. D **65**, 092007 (2002).

[6] R. Bernabei et al., Phys. Lett. B **546**, 23 (2002).

[7] F.A. Danevich et al., Phys. Rev. C **68**, 035501 (2003).

[8] E. Andreotti et al., Astropart. Phys. **34**, 822 (2011).

[9] A.S. Barabash, V.B. Brudanin and NEMO Collaboration, Phys. At. Nucl. **74**, 312 (2011).

[10] H.V. Klapdor-Kleingrothaus, I.V. Krivosheina, Mod. Phys. Lett. A **21**, 1547 (2006).

[11] A.S. Barabash et al., J. Phys. G **34**, 1721 (2007).

[12] H.J. Kim et al., Nucl. Phys. A **793**, 171 (2007).

[13] A.S. Barabash et al., Nucl. Phys. A **807**, 269 (2008).

[14] J. Dawson et al., Nucl. Phys. A **799**, 167 (2008).

[15] P. Belli et al., Phys. Lett. B **658**, 193 (2008).

[16] P. Belli et al., Eur. Phys. J. A **36**, 167 (2008).

[17] A.S. Barabash et al., Phys. Rev. C **80**, 035501 (2009).

[18] P. Belli et al., Eur. Phys. J. A **42**, 171 (2009).

[19] P. Belli et al., Nucl. Phys. A **824**, 101 (2009).

[20] P. Belli et al., Nucl. Phys. A **826**, 256 (2009).

[21] Yu.M. Gavrilyuk et al., Bull. Rus. Ac. Sci. Physics **75**, 526 (2011).

[22] N.I. Rukhadze et al., Nucl. Phys. A **852**, 197 (2011).

[23] N.I. Rukhadze et al., Bull. Rus. Ac. Sci. Physics **75**, 879 (2011).

[24] P. Belli et al., J. Phys. G **38**, 015103 (2011).

[25] E. Andreotti et al., Astropart. Phys. **34**, 643 (2011).

[26] A.S. Barabash et al., Phys. Rev. C **83**, 045503 (2011).

[27] P. Belli et al., J. Phys. G **38**, 115107 (2011).

[28] A.P. Meshik et al., Phys. Rev. C **64**, 035205 (2001).

[29] M. Pujol et al., Geochim. Cosmochim. Acta **73**, 6834 (2009).

[30] R. Cerulli et al., Nucl. Instr. Meth. A **525**, 535 (2004).

[31] M. Hirsch et al., Z. Phys. A **347**, 151 (1994).

[32] M. Goncharov et al., Phys. Rev. C **84**, 028501 (2011).

[33] M. Berglund and M.E. Wieser, Pure Appl. Chem. **83**, 397 (2011).

[34] A. Staudt, K. Muto, and H.V. Klapdor-Kleingrothaus, Phys. Lett. B **268**, 312 (1991).

[35] J. Toivanen and J. Suhonen, Phys. Rev. C **55**, 2314 (1997).

[36] S. Stoica and H.V. Klapdor-Kleingrothaus, Eur. Phys. J. A **17**, 529 (2003).

[37] A. Shukla et al., Eur. Phys. J. A **23**, 235 (2005).

[38] P. Domin et al., Nucl. Phys. A **753**, 337 (2005).

[39] A.S. Barabash et al., Nucl. Phys. A **604**, 115 (1996).

[40] O.A. Rumyantsev and M.H. Urin, Phys. Lett. B **443**, 51 (1998).

[41] O. Civitarese and J. Suhonen, Phys. Rev. C **58**, 1535 (1998).

[42] J. Suhonen and O. Civitarese, Phys. Lett. B **497**, 221 (2001).

[43] R.G. Winter, Phys. Rev. **100**, 142 (1955).

[44] M.B. Voloshin, G.V. Mitselmakher, and R.A. Eramzhyan, JETP Lett. **35**, 656 (1982).

[45] J. Bernabeu, A. de Rujula, and C. Jarlskog, Nucl. Phys. B **223**, 15 (1983).

[46] Z. Sujkowski and S. Wycech, Acta Phys. Pol. B **33**, 471 (2002).

[47] Z. Sujkowski and S. Wycech, Phys. Rev. C **70**, 052501 (2004).

[48] M.I. Krivoruchenko et al., Nucl. Phys. A **859**, 140 (2011).

[49] J.H. Fremlin and M.C. Walters, Proc. Phys. Soc. Lond. A **65**, 911 (1952).

[50] R.G. Winter, Phys. Rev. **99**, 88 (1955).

[51] E.B. Norman and M.A. DeFaccio, Phys. Lett. B **148**, 31 (1984).

[52] D. De Frenne and A. Negret, Nuclear Data Sheets **109**, 943 (2008).

[53] P. Belli et al., Astropart. Phys. **10**, 115 (1999).

[54] Y. Ito et al., Nucl. Instr. Meth. A **386**, 439 (1997).

[55] J.V. Dawson et al., Phys. Rev. C **80**, 025502 (2009).

[56] A.Sh. Georgadze et al., Phys. At. Nucl. **58**, 1093 (1995).

[57] F.A. Danevich et al., Z. Phys. A **355**, 433 (1996).

[58] F.A. Danevich et al., Phys. Atom. Nucl. **59**, 1 (1996).

[59] F.A. Danevich et al., Phys. Rev. C **67**, 014310 (2003).

[60] P. Belli et al., Phys. Rev. C **76**, 064603 (2007).

[61] P. Belli et al., Nucl. Instr. Meth. A **615**, 301 (2010).

[62] R.S. Boiko et al., Inorganic Materials **47**, 645 (2011).

[63] P. Belli et al., Proc. Int. Conf. NPAE-2010, 7-12 June 2010, Kyiv, Ukraine – Kyiv, 2011, p. 428;
P. Belli et al., AIP Conf. Proc. **1304**, 354 (2010).

[64] N.I. Rukhadze et al., Phys. At. Nucl. **69**, 2117 (2006).

[65] F.A. Danevich et al., Phys. Lett. B **344**, 72 (1995).

[66] F.A. Danevich et al., Nucl. Phys. A **694**, 375 (2001).

[67] R.B. Firestone et al., *Table of Isotopes*, 8-th ed., John Wiley, New York, 1996 and CD update, 1998.

[68] T. Fazzini et al., Nucl. Instr. Meth. A **410**, 213 (1998).

[69] E. Gatti, F. De Martini, Nuclear Electronics 2, IAEA, Vienna, 1962, p. 265.

[70] L. Bardelli et al., Nucl. Instr. Meth. A **569**, 743 (2006).

[71] P. Belli et al., Nucl. Phys. A **789**, 15 (2007).

[72] G. Bellini et al., Eur. Phys. J. C **19**, 43 (2001).

[73] A.S. Barabash et al., JINST **6**, P08011 (2011).

[74] W.R. Nelson et al., SLAC-Report-265, Stanford, 1985.

[75] S. Agostinelli et al., Nucl. Instr. Meth. A **506**, 250 (2003);
J. Allison et al., IEEE Trans. Nucl. Sci. **53**, 270 (2006).

[76] O.A. Ponkratenko et al., Phys. At. Nucl. **63**, 1282 (2000);
V.I. Tretyak, to be published.

[77] R. Bernabei et al., Il Nuovo Cim. A **112**, 545 (1999).

[78] M. Günther et al., Phys. Rev. D **55**, 54 (1997).

[79] P. Belli et al., Nucl. Instr. Meth. A **626-627**, 31 (2011).

[80] A. Balysh et al., Pribory i Tekhnika Eksperimenta **1**, 118 (1993) (in Russian).

[81] P. de Marcillac et al., Nature **422**, 876 (2003).

[82] N. Coron et al., Proc. Workshop Radiopure Scint. for EURECA (RPScint'2008), arXiv:0903.1539 [nucl-ex], p. 12.

[83] D.N. Grigoriev et al., Nucl. Instr. Meth. A **623**, 999 (2010).

[84] H.V. Klapdor-Kleingrothaus et al., Phys. Rev. D **55**, 54 (1997).

[85] G.J. Feldman, R.D. Cousins, Phys. Rev. D **57**, 3873 (1998).

[86] J. Suhonen, Phys. Lett. B **701**, 490 (2011).

[87] J. Suhonen and O. Civitarese, Phys. Rep. **300**, 123 (1998).

[88] J. Suhonen, Nucl. Phys. A **563**, 205 (1993).

[89] O. Civitarese and J. Suhonen, Nucl. Phys. A **575**, 251 (1994).

[90] M. Kortelainen et al., Phys. Lett. B **647**, 128 (2007).

[91] F.A. Danevich et al., Nucl. Instr. Meth. A **603**, 328 (2009).

[92] A.V. Tikhomirov, private communication.